# REPORT DOCUMENTATION PAGE

*Form Approved*
*OMB No. 0704-0188*



| 1. REPORT DATE *(DD-MM-YYYY)* | 2. REPORT TYPE | 3. DATES COVERED *(From - To)* |
|---|---|---|
| 07-10-2009 | Technical Paper | |

**4. TITLE AND SUBTITLE**

**Assessment of BGK Approaches to Modeling of Nozzle Flows (PREPRINT)**

**5a. CONTRACT NUMBER**

**5b. GRANT NUMBER**

**5c. PROGRAM ELEMENT NUMBER**

**6. AUTHOR(S)**
R. Kumar, E.V. Titov, and D.A. Levin (Penn State); N.E. Gimelshein and S.F. Gimelshein (ERC)

**5d. PROJECT NUMBER**

**5e. TASK NUMBER**

**5f. WORK UNIT NUMBER**
**23080532**

**7. PERFORMING ORGANIZATION NAME(S) AND ADDRESS(ES)**

Air Force Research Laboratory (AFMC)
AFRL/RZSA
10 E. Saturn Blvd.
Edwards AFB CA 93524-7680

**8. PERFORMING ORGANIZATION REPORT NUMBER**

AFRL-RZ-ED-JA-2009-361

**9. SPONSORING / MONITORING AGENCY NAME(S) AND ADDRESS(ES)**

Air Force Research Laboratory (AFMC)
AFRL/RZS
5 Pollux Drive
Edwards AFB CA 93524-7048

**10. SPONSOR/MONITOR'S ACRONYM(S)**

**11. SPONSOR/MONITOR'S NUMBER(S)**
AFRL-RZ-ED-JA-2009-361

**12. DISTRIBUTION / AVAILABILITY STATEMENT**

Approved for public release; distribution unlimited (PA #09446).

**13. SUPPLEMENTARY NOTES**
For publication in Journal of Computational Physics in 2010.

**14. ABSTRACT**

Accurate and numerically efficient modeling of low to moderate Reynolds number nozzle flow expansions to vacuum can be difficult due to the presence of multiple flow length scales. Such simulations are important for the prediction of propulsive thrust as well as spacecraft contamination, both of which can be difficult to measure in ground based facilities. To that end, conical nozzle flows were studied for Reynolds numbers of 1,230 and 12,300 using the direct simulation Monte Carlo method (DSMC), Navier-Stokes with velocity slip and temperature jump boundary conditions, and statistical and deterministic approaches to the solution of the BGK and ES-BGK equations. The deterministic and statistical solutions of the BGK equation were found to be in good agreement with the benchmark DSMC results. Statistical BGK and ES-BGK methods were also found to be more efficient methods than DSMC in the continuum and near-continuum regime, and more accurate than the Navier-Stokes equations in the portions of the flow with rarefaction, such as the boundary layer and the flow around the nozzle lip.

**15. SUBJECT TERMS**

| 16. SECURITY CLASSIFICATION OF: | | | 17. LIMITATION OF ABSTRACT | 18. NUMBER OF PAGES | 19a. NAME OF RESPONSIBLE PERSON |
|---|---|---|---|---|---|
| | | | | | Ingrid Wysong |
| a. REPORT | b. ABSTRACT | c. THIS PAGE | SAR | 28 | 19b. TELEPHONE NUMBER *(include area code)* |
| **Unclassified** | **Unclassified** | **Unclassified** | | | N/A |

# Assessment of BGK Approaches to Modeling of Nozzle Flows in the Near Continuum Regime

Rakesh Kumar*, E. V. Titov† and D. A. Levin‡
*Pennsylvania State University, University Park, PA 16802*
N. E. Gimelshein§ and S. F. Gimelshein¶
*ERC, Inc., Edwards AFB, CA 93524*

**Accurate and numerically efficient modeling of low to moderate Reynolds number nozzle flow expansions to vacuum can be difficult due to the presence of multiple flow length scales. Such simulations are important for the prediction of propulsive thrust as well as spacecraft contamination, both of which can be difficult to measure in ground based facilities. To that end, conical nozzle flows were studied for Reynolds numbers of 1,230 and 12,300 using the direct simulation Monte Carlo method (DSMC), Navier-Stokes with velocity slip and temperature jump boundary conditions, and statistical and deterministic approaches to the solution of the BGK and ES-BGK equations. The deterministic and statistical solutions of the BGK equation were found to be in good agreement with the benchmark DSMC results. Statistical BGK and ES-BGK methods were also found to be more efficient methods than DSMC in the continuum and near-continuum regime, and more accurate than the Navier-Stokes equations in the portions of the flow with rarefaction, such as the boundary layer and the flow around the nozzle lip.**

*Graduate Student, Department of Aerospace Engineering.
†Postdoctoral Researcher, Department of Aerospace Engineering, AIAA member.
‡Professor, Department of Aerospace Engineering, AIAA Associate Fellow.
§Aerospace Engineer, Edwards AFB.
¶Aerospace Engineer, Edwards AFB.

*Nomenclature

| | | |
|---|---|---|
| $\delta_{ij}$ | : | Kronecker delta |
| $\mu$ | : | Dynamic viscosity |
| $\mu_{ref}$ | : | Reference dynamic viscosity |
| $\nu$ | : | Characteristic relaxation frequency |
| $\rho$ | : | Density |
| $\Omega$ | : | Solid angle |
| $\omega$ | : | Viscosity temperature index |
| $\sigma$ | : | Differential cross-section of the binary collision |
| D | : | Nozzle throat diameter |
| FV | : | Finite volume |
| f | : | Single particle velocity distribution function |
| $f_e$ | : | Maxwellian distribution function |
| $f_G$ | : | Ellipsoidal-Statistical distribution function |
| $\vec{F}$ | : | External force per unit mass |
| k | : | Boltzmann constant |
| m | : | Mass of a molecule |
| N | : | Number of particles in a cell |
| $N_c$ | : | Number of particles selected for velocity resampling |
| n | : | Number density |
| Pr | : | Prandtl number |
| p | : | Internal pressure |
| $\vec{r}$ | : | Radial vector |
| R1,R2 | : | Random numbers |
| Re | : | Reynolds number |
| $S_{ij}$ | : | Modifying tensor |
| T | : | Local temperature in a cell |
| To | : | Stagnation temperature |
| $T_{ref}$ | : | Reference temperature |
| t | : | Time |
| U* | : | Sonic velocity at the nozzle throat |
| $\vec{v}$ | : | Velocity vector |
| $v_r$ | : | Relative velocity of the colliding particles |
| $v_i$ | : | Velocity vector in Cartesian coordinates |

# I. Introduction

Nozzle flows at low and moderate Reynolds numbers are characterized by multiple flow length scales, which significantly complicates their accurate and numerically efficient modeling. Multiparameteric analysis of such flows is also problematic due to a large number of cases that need to be examined for the optimization of the nozzle based device performance. Experimental studies under such conditions are rare, expensive (particularly for microscale, MEMS flows), and may not provide the necessary accuracy in the measurement of the principal nozzle characteristics such as thrust, flow rate, and specific impulse.[1] For both micro and meso-sized nozzles operating in the space near-vacuum environment, the interaction with critical spacecraft surfaces at high altitudes needs to be analyzed. Back-flow produced by such devices plays a major role in the contamination to sensitive electronic devices such as optical instruments and solar panels, which in turn may adversely affect the life span of spacecraft.[2,3] The back-flow formation is very sensitive to the conditions at the nozzle lip, and is difficult to study in ground based facilities, particularly for micro-nozzle flows.[4] For the International Space Station, the control thruster exhaust products turn out to be the most important agents of contamination. The contamination of such electronic devices on a spacecraft can become mission critical by significantly reducing its active life span.[4] Therefore, in the present work, we carried out nozzle supersonic expansion to vacuum studies with the goal of studying the core flow as well as flow reversal rate differences among the statistical and deterministic ES-BGK and Navier-Stokes (NS) methods. The baseline direct simulation Monte Carlo (DSMC) method is utilized as the basis for comparison for the aforementioned gas dynamic approaches. The numerical accuracy can be well characterized for DSMC, as will be discussed, but it is too computationally intensive for the range of conditions necessary to analyze micro-nozzle thrust and spacecraft contamination. Therefore, in the comparison among the gas dynamic techniques, computational efficiency will also be addressed.

The development of accurate numerical tools capable of simulating micro-nozzle flows is important, but at the same time, challenging, because the flow regime changes from continuum, near the nozzle throat, to transitional at the nozzle exit. Kinetic methods, such as DSMC, and continuum techniques based on the solution of the NS equations, encounter computational constraints and physical challenges when applied to these flows. The principal problem with the DSMC method[5] is the associated computational cost when high density portions of the flow have to be accurately modeled. This is essentially due to the large number of collisions in the high density regime, in addition to the usual constraints of cell size and time step being of the order of mean free path and mean collision time, respectively. On the other hand, conventional continuum CFD techniques are inapplicable in flow regions of high gradients and strong rarefaction even when velocity slip and temperature jump

boundary conditions are imposed at the nozzle surface. These factors become paramount at the exit of the nozzle for supersonic expansions to vacuum, but, can even be seen in supersonic expansions to non-vacuum, finite back pressures.[6] Attempts to correct the NS equations through the use of the Burnett equations for micronozzle flow modeling showed that the latter are in better agreement with DSMC, but only up to Knudsen numbers of approximately 0.2.[7]

In recent years, combined but uncoupled NS/DSMC approaches have been often used to model nozzle flows in the transitional Knudsen number regime,[8,9] where the NS equations were used to model the high density portions of the flow inside the nozzle, and the DSMC method was used to predict the rarefied plume-atmosphere interaction. A starting surface was used to transfer the properties obtained in the continuum portion of the flow to the DSMC solver. The flow was always assumed to be in the steady state, and the uncoupled approach implied that the more rarefied, DSMC portions of the flow have negligible effect on the continuum portions. This approach, however, becomes problematic when the implicit assumptions are violated, for example, when the hand-off surface is in a subsonic region, or the downstream flow affects the upstream flow through radiation, or the flow geometry is three-dimensional and complicated. La Toree *et al*[10] recently used DSMC, NS, and coupled-hybrid DSMC/NS approaches to evaluate micronozzle performance for expansions to vacuum and found the macroparameter distributions to be sensitive to the location of the interface between the two methods.

To overcome this problem, it is possible to use a two-way coupled hybrid continuum-kinetic approach (see, for example, Refs. 11–13), where the interface location can be dynamically varied during the simulation by evaluating continuum breakdown parameters. However, an accurate determination of the interface boundary demands additional computational effort. There will also be the usual hybridization problems[14] and, moreover, the extension to chemically reacting flows, i.e., to flows consisting of species with significant internal energy, or to two-phase models may not be straightforward. The deficiencies in the implementation of a hybrid NS-DSMC approach become even more problematic when transient nozzle and plume flows need to be analyzed. The main difficulty is related to the temporal changes in gas properties: most importantly gas mean free path and the Mach number, that necessitate flexible, transient hand-off surfaces and interface boundaries.

Considering the aforesaid difficulties in modeling nozzle flows in the transition regime, it would be desirable to have a single method that allows an accurate and efficient one-step modeling of high density nozzle and low density plume flows. Recent years have witnessed a renewed interest and significant advances in the solution of model kinetic equations such as BGK,[15] BGK/ES-BGK,[16] with deterministic, either finite difference or finite volume, approaches typically used in the solution procedure. A particle approach to obtain the

solution to the BGK equation was first proposed in Ref. 17. It was then extended to model the ES-BGK equation in Ref. 16, and further extended to include rotational degrees of freedom in Ref. 18. The general idea behind the use of model kinetic equations as replacement for DSMC is that the solution of the former will be more efficient than DSMC in the continuum and near-continuum regimes, and more accurate than the solution of the NS equations in the transitional regions of the flow.

With respect to nozzle flows, one of first attempts to use model kinetic equations is the work of Burt *et al*[18] where a statistical, particle approach to the solution of the ES-BGK equation was obtained for a flow expanding through a conical nozzle. More recently their work[19] was extended to combine the advantages of the NS and DSMC approaches. In the low diffusion particle method the viscosity is modeled by computing the diffusive terms in the compressible NS equations in the equilibrium regions of the flow whereas the DSMC procedure is used in the nonequilibrium regions. Although initially successful, the refinement of the method to realistic, more complex flows including internal degrees of freedom and chemistry still remains. In our earlier work,[20] we developed and studied a statistical technique, that models continuum flows using a collision enforcement procedure to guarantee full relaxation of the particle thermal velocities to a state of local equilibrium, hence the name, "eDSMC." The technique was applied to internal flows for nozzles as well as channels and compared well with nozzle data and previous channel calculations. The technique was shown to be able to solve inviscid flows with tangency (or specular) wall boundary conditions (*i.e.,* Eulerian), but under predicted viscous effects in the boundary layer when diffuse gas-wall boundary conditions were used.

In the present work, we continue our efforts to apply statistical methods to moderate and high Reynolds number nozzle flows by making use of the BGK[15] and ES-BGK models.[21] A particular goal is to understand the benefits of the particle BGK/ES-BGK approaches as compared to the conventional DSMC method. For BGK/ES-BGK approaches to be competitive with DSMC, it must be understood if the standard DSMC requirements can be relaxed. If so, this would then allow BGK/ES-BGK models to be used for high pressure cases, where the DSMC method is impractical due to the required computational resources. As it will be shown in Sec. III, the use of NS method is not a good alternative for supersonic expanding flows to vacuum. We compare numerical simulations for transitional nozzle flows expanding into a vacuum using five different numerical approaches - DSMC, finite volume and particle solutions of the BGK and ES-BGK model kinetic equations, solution of the NS equations and an equilibrium DSMC (eDSMC) technique for two test cases corresponding to Reynolds numbers of 1,230 and 12,300. Such comparisons of the model kinetic equation approaches with the formally derived computational schemes such as DSMC and NS are rarely found in a single article and will allow us to assess the utility of the particle BGK and

ES-BGK approaches as stand alone procedures. Moreover, in future work it may be possible to utilize the best possible features of the particle-statistical BGK and DSMC methods in terms of numerical efficiency and accuracy to construct a particle-particle hybrid method consisting of these two methods.

The remainder of the paper is as follows. In Sec. II we outline the theory and our method of implementation of the computational approaches that are used. We discuss the numerical parameters selected for the DSMC calculations since this baseline method will be used to model a high pressure case, usually outside the typical practical region for most DSMC calculations. In Sec. III we discuss the numerical parameters chosen for the BGK/ES-BGK calculations to minimize statistical errors so that small differences among the methods can be seen. Macroparameters such as gas density, temperature, and velocity along the nozzle centerline and across the nozzle exit are compared, as well as back flow regions downstream of the nozzle exit. To compare the numerical efficiency of the methods, the rationale for a new set of numerical parameters is discussed and employed. In addition, boundary layer growth and flow averaged quantities such as thrust and back flow rates are compared. Conclusions are presented in Sec. IV.

## II. Computational Methods

### II.A. DSMC Method

The simulation of rarefied flows is typically performed using the DSMC approach, a discrete particle simulation method that approximates a numerical solution to the Boltzmann equation. DSMC achieves computational efficiency by decoupling, in time, the movement and collisions of molecules. Simulated particles, each representing a large number of real atoms/molecules, are moved, tracked through the computational mesh, and are indexed and sorted into cells according to their locations. During each time step, some fraction of the particles in a cell collide with each other, and probabilistic techniques are used to evaluate the outcome of individual collisions. The colliding particles are assigned new velocities according to the specified interaction law, so that the energy and momentum are conserved, and are then moved through the mesh at the assigned velocities. Boundary conditions are modeled through collisions of the computational particles with the surfaces by properly choosing the gas-surface interaction parameters. Macroparameters are obtained by the appropriate summation over all the particles contained in the cells.[5]

The DSMC-based SMILE (Statistical Modeling in a Low Density Environment) computational solver is used in this work. The solver has both 2D and axisymmetric capabilities. The important features that are used in the present work include the axisymmetric capability with radial weights, different grids for collisions and macroparameters, both of which are

two-level adaptable Cartesian grids, and parallel implementation with efficient load balancing techniques.[22] The physical space is modeled in a cylindrical coordinate system, while the velocity space is 3-D Cartesian. The majorant frequency scheme of Ivanov and Rogasinsky[23] is employed for modeling gaseous species collisions and the Variable Hard Sphere (VHS)[5] model is used for modeling the total collision cross-section. Diffuse reflection with full thermal accommodation is assumed at the nozzle wall. For both Reynolds numbers, solutions independent of grid, time step, and number of particles are obtained. For Re=1,230 (Case I, see Table 1), there is virtually no difference observed between solutions obtained for 0.47 million cells with 5 million simulated molecules, and 3 million cells with 30 million simulated molecules. For Re=12,300 (Case II, see Table 2), this is true for numerical parameters up to an order of magnitude larger. Tables 1 and 2 provide a summary of the numerical parameters used for the two cases considered in this work. The DSMC and BGK simulations are accurate to within 2%. The eDSMC calculations discussed in Sec. III.B were computed using 0.85 million cells with 5 million particles.

### II.B. Solution of the NS Equations

The commercial code, CFD++,[24] has been used in this work to solve the NS equations. CFD++ is a flexible computational fluid dynamics software suitable for the solution of the steady and unsteady, compressible and incompressible NS equations, and includes a multi-species capability for perfect and reacting gases. In this work, a perfect-gas compressible NS solver is used with second order spatial discretization and implicit time integration. Second order velocity slip and temperature jump conditions are imposed on the nozzle wall. A supersonic inflow with prescribed parameters is applied at the nozzle throat, and backpressure of 1 Pa is imposed at the outflow boundaries. A symmetry condition is defined at the nozzle axis. The results presented below (both flow fields and computational requirements) are obtained for a multi-block rectangular grid with a total of 14,400 nodes. The computations are also conducted for four times smaller and four times larger numbers of nodes, and found to be fully grid-resolved with 14,400 nodes.

### II.C. Solution of the BGK Equation

The velocity distribution function provides a full description of a gas at the molecular level. The relationship for the velocity distribution function is given by the Boltzmann equation:

$$\frac{\partial}{\partial t}(nf) + \vec{v} \cdot \frac{\partial}{\partial \vec{r}}(nf) + \vec{F} \cdot \frac{\partial}{\partial \vec{v}}(nf) = \left[\frac{\partial}{\partial t}(nf)\right]_{collision} \tag{1}$$

where $f$ is the single particle velocity distribution function, $n$ is the number density, $\vec{F}$ is an external force per unit mass that applies to the particles (assumed to be zero for the present study). The term on the right hand side is the collision term and is given by the following equation:

$$\left[\frac{\partial}{\partial t}(nf)\right]_{collision} = \int_{-\infty}^{\infty}\int_{0}^{4\pi} n^2\left(f^* f_1^* - f f_1\right) v_r \sigma d\Omega d\vec{v} \tag{2}$$

where $f$ and $f_1$ are the values of the velocity distribution function at pre-collision velocities of the two colliding particles and $f^*$ and $f_1^*$ are the corresponding values at post-collision velocities; $\sigma$ is the differential cross-section of the binary collision, $\Omega$ is the solid angle and $v_r$ is the relative velocity of the colliding particles. It is clear that the collision term involves multiple integrations in its analytical formulation, and is therefore difficult to compute. Hence different simplified models have been introduced to model the inherently complicated collision term of the Boltzmann equation. One such simplified model is from Bhatnagar, Gross and Krook,[15] that approximates the collision term as follows:

$$\left[\frac{\partial}{\partial t}(nf)\right]_{collision} = \nu n(f_e - f) \tag{3}$$

where $n$ is the number density, $\nu$ is the characteristic relaxation frequency and $f_e$ is the Maxwellian distribution function. In this model, the nonlinear collision term in the Boltzmann equation is approximated by a Maxwellian molecular model in which the distribution function $f$ proceeds toward local equilibrium at a velocity independent rate. Thus the BGK method provides an alternate procedure to account for the collisional process driving a flow toward equilibrium without modeling individual collisions. The idea behind this simplification is that the intricate details of the two-body interactions are not important in reproducing most of the experimentally measured macroscopic quantities such as temperature, pressure or flow velocity, if the collision rate is sufficiently high.[16]

The BGK equation reproduces correct moments and satisfies the H-theorem for entropy production. In Eq. 3, the term $n\nu f_e$ represents the collisions replenishing the local Maxwellian equilibrium distribution $f_e$, and the term $n\nu f$ represents the collisions depleting the molecules out of existing distribution $f$.[16] There are arguments about the importance and the specifics of algorithms to preserve energy and momentum conservation, which, in the opinion of the authors is a secondary problem, since, on average, these quantities are preserved. The major issue seems to be the absence of the formal derivation of the numerical schemes from the BGK equation, in a similar manner as it is conducted for DSMC schemes.[23] For this reason, the simulation results of BGK methods presented in Sec. III will be compared with the DSMC method. The BGK equation is solved by both statistical and finite volume methods in the present work.

*II.C.1. Statistical Method for Solution of the BGK Equation*

Recently, a number of authors[16,18,25] have developed particle approaches to the solution of the BGK equations. While these approaches differ in details and the arguments regarding the formal connection between the numerical schemes and the equations continue, the basic ideas of the numerical schemes remain the same. Instead of selecting collision pairs from all of the simulated particles, a fraction of particles are randomly selected during each time step from those available in a computational cell, and are assigned new velocities according to local Maxwellian (BGK) or ellipsoidal (ES-BGK) distribution functions. If the collision frequency for such a velocity reassignment is properly computed and the local values of the translational temperature in the cells are known, then the procedure certainly mimics the collision term on the right hand side of the BGK equation given by Eq. 3.

**Statistical BGK Method**

Since the only difference between the DSMC method and a particle solution of the BGK equation lies in the modeling of the collision term, procedures other than intermolecular collisions in the BGK particle method are identical to those in DSMC method. The details of the statistical BGK model are as follows:[16–18]

The characteristic relaxation/collision frequency is calculated as

$$\nu = \Pr \cdot nk \left( \frac{T_{ref}^{\omega}}{\mu_{ref}} \right) T^{1-\omega} \tag{4}$$

where Pr is the Prandtl number (1 for the BGK equation), $k$ is the Boltzmann constant, $T$ is the local translational temperature in a cell, $\omega$ is the viscosity temperature index and $\mu_{ref}$ is the gas dynamic viscosity at $T_{ref}$. The collision frequency is calculated for each computational cell at each time step based on the local translational temperature $T$ and the local number density $n$. The local number density $n$ is averaged over a large number of computational time steps, while the local temperature $T$ is computed based on the instantaneous thermal velocities of the computational particles in the cell.

The number of particles preselected for velocity resampling, i.e., particles for which velocities are reassigned according to the local Maxwellian distribution, is calculated as follows:

$$N_c = \text{int}(N(1 - \exp(-\nu \Delta t)) \tag{5}$$

where $N$ is the number of particles in a cell, $\Delta t$ is the time step, and *int* operator means the nearest smaller integer. To compensate for the systematic error that such an operator produces, one more particle is added to to the list of preselected particles with the probability:

$$P_c = N(1 - \exp(-\nu\Delta t) - \mathrm{int}(N(1 - \exp(-\nu\Delta t)) \tag{6}$$

The preselected particles receive new velocities, $\overrightarrow{v^1}$, according to the local Maxwellian distribution. Each velocity component is set via

$$v_x^1 = \cos(2\pi R_1)\sqrt{-\ln(R_2)} \cdot \sqrt{2kT/m} \tag{7}$$

$$v_y^1 = \sin(2\pi R_1)\sqrt{-\ln(R_2)} \cdot \sqrt{2kT/m} \tag{8}$$

$$v_z^1 = \cos(2\pi R_3)\sqrt{-\ln(R_4)} \cdot \sqrt{2kT/m} \tag{9}$$

where $R_1$ through $R_4$ are random numbers uniformly distributed between 0 and 1. The velocities of particles that have not been preselected remain unchanged in the current time step.

**Statistical ES-BGK Method**

The BGK model has an inherent property that Prandtl number is unity for all cases. This may be a source of error for cases in which the thermal conductivity plays an important role. Holway[26] and Cercignani[27] proposed a modification to the BGK equation that ensures the correct production of transport coefficients similar to the Boltzmann equation, and has been recently shown to satisfy Boltzmann's H-theorem for entropy production.[28] The ES-BGK model is obtained by the replacement of the Maxwellian distribution with a local anisotropic three-dimensional Gaussian, referred to as the Ellipsoidal-Statistical (ES) model:

$$\left[\frac{\partial}{\partial t}(nf)\right]_{collision} = \nu n(f_G - f) \tag{10}$$

The procedure of calculating the characteristic relaxation frequency (with the physically correct Prandtl number), selection and resampling of velocities for a fraction of particles available in a computational cell are the same as in the statistical BGK method. However after resampling of all velocity components, $\overrightarrow{v^1}$, they are modified to $\overrightarrow{v^2}$ in order to conform to the ES distribution:

$$v_i^2 = S_{ij} \cdot v_j^1 \tag{11}$$

where $\overrightarrow{v^2}$ designates the modified velocity components and $S_{ij}$ is given by the following equation:

$$S_{ij} = \delta_{ij} - \frac{1 - Pr}{2Pr}\left[\frac{1}{kT}\frac{N}{N-1}\left(< mv_iv_j >_a - < mv_i >_a < mv_j >_a / < m >_a\right) - \delta_{ij}\right] \tag{12}$$

where the symbol $<>_a$ represents an averaging over all the particles in a cell, $\delta_{ij}$ is the Kronecker delta, and $m$ is the mass of a particle.

### II.D. Finite Volume Method for Solution of the BGK/ES-BGK Equation

A finite volume solver SMOKE developed at ERC, Inc., has been used to deterministically solve the BGK and ES-BGK equations. SMOKE is a parallel code based on numerical schemes developed by L. Mieussens.[29] Both implicit and explicit time integration schemes are implemented. The time-accurate explicit schemes are constructed to strictly satisfy mass, momentum, and energy conservation requirements, while the implicit schemes do not have this advantage. Nevertheless, for the problem under consideration it was found that the implicit schemes provide adequate accuracy, and subsequent application of the explicit schemes essentially does not visibly change the flowfields. The results obtained by implicit schemes are therefore shown below.

The code has both 2D and axisymmetric capabilities, with the latter one used in this work. A second order axisymmetric spatial discretization is used along with the first order velocity ($v_x$, $v_r$, $v_\theta$) discretization. Here $v_x$ is the velocity component along $x$ direction, $v_r$ the radial component, and $v_\theta$ completes the right handed system. Note that the coordinate system used in the finite volume scheme is different from that used in the statistical BGK method, where Cartesian components, $v_x$, $v_y$, $v_z$, were used instead. A supersonic inflow condition is used at the nozzle throat, and vacuum outflow conditions are set at the outer boundaries. Fully diffuse reflection with complete energy accommodation is applied at the nozzle surface. The spatial grid convergence was achieved by increasing the number of nodes from 3,600 to over 17,000. The convergence on the velocity grid was also studied, with the number of grid points ranging from (20,10,18) to (30,35,50).

## III. Results and Discussion

A gas flow of argon through a conical nozzle expanding into a vacuum is considered in this work. The diverging portion of the nozzle is modeled, and its geometry is taken from Ref. 30. The nozzle throat diameter is 2.5 mm, the length of the diverging part is 50.7 mm, and the half-angle is 20°. The surface temperature of the nozzle is assumed to be 300 K. The numerical results are obtained for two throat-diameter based Reynolds numbers of 1,230 and 12,300, with a stagnation temperature of 333.33 K. The respective flow Knudsen numbers are $1.59\text{x}10^{-3}$ and $1.59\text{x}10^{-4}$, where the mean free path has been calculated for the stagnation conditions. In all numerical approaches, the computational domain starts at the nozzle throat and covers the entire diverging part of the nozzle, as well as a small part of the plume to avoid the influence of the downstream boundary conditions.[31] Four different

numerical approaches are used, as explained in the last section.

We compare the results of the statistical BGK/ES-BGK methods with those of the finite volume solution to the same equation and the DSMC method. In order to reduce the statistical error so that small differences among the different kinetic methods may be studied, a large number of simulated particles were used such that the minimum number of particles per cell is about 150. This unusually large number of particles per cell also provides a better statistical approximation of the local instantaneous cell based temperature and more accurate conservation of momentum and energy.[16]

Since the specific advantages of statistical BGK and ES-BGK methods over other methods is of interest, a comprehensive sensitivity study is carried out with respect to cell size/time step and number of particles in a cell.

### III.A. Low pressure Case I

Results for the low pressure Case I were obtained by the baseline DSMC Smile[22] code, a modified version that implements the statistical BGK and ES-BGK scheme, a finite volume ES-BGK solver, and a Navier-Stokes solver.[24] The DSMC method is understood to provide the most accurate solution for this case, as the conditions are well within the range where a mesh converged DSMC solution is obtainable and all of the strict DSMC method criteria (as described in Sec. II.A) are satisfied during the calculation. Since temperature is the most sensitive parameter in BGK model due to the constraint of Prandtl number equal to unity, we show temperature contour plots for the different methods for the purpose of comparison. In all the figures, temperature is normalized by the stagnation temperature of the flow (333.33 K), flow velocity is normalized by the sonic velocity at the nozzle throat (294.55 m/s), density is normalized by the density at the nozzle throat (0.013989 kg/m$^3$), x and y coordinates are normalized by the throat diameter (2.5 mm) of the nozzle, $x/D = 0$ corresponds to the nozzle throat and $y/D = 0$ corresponds to the nozzle centerline.

The general flow physics of supersonic expansions to vacuum are illustrated in Fig. 1 which shows a comparison of temperature contours predicted by the DSMC, ES-BGK, and NS approaches. All gas dynamic methods show the typical structure of an inviscid flow core as well as the development of a thick, viscous boundary layer. The predicted flow structure for the ES-BGK agrees best with the DSMC, whereas, the NS shows the poorest agreement of all the gas dynamic techniques. The other gas dynamic techniques show similar qualitative agreement with DSMC compared to the ES-BGK method, and, subtle differences will be illustrated in linear profiles discussed below.

To quantify the differences among the different numerical methods, selected flow parameters are presented along the nozzle centerline (Fig. 2) and across the nozzle at the exit plane (Fig. 3) for all of the methods. Figure 2 shows that all gas dynamic approaches agree well

within the core of the flow predicting virtually identical density, velocity, and temperature profiles for similar to (but not the same as) isentropic expansions. Important difference among the techniques, however, can be seen in Fig. 3 the most likely portion of the flow where differences could occur, *i.e.*, the expansion of the boundary layer over the nozzle lip. Figure 3 shows that the statistical BGK scheme deviates slightly from DSMC close to the wall at the nozzle exit plane. The results obtained by the statistical ES-BGK scheme match well with those of DSMC and FV ES-BGK method along the nozzle centerline and exit plane. The FV ES-BGK scheme agrees well with the DSMC method, with small deviations from it close to the nozzle exit towards the nozzle wall. Generally, FV ES-BGK method can be expected to be close to NS for larger Reynolds number, and somewhere between DSMC and NS for smaller Reynolds number. The reason for this is the limitations posed by the ES-BGK equation itself, wherein the collision term limits ES-BGK applicability to highly nonequilibrium flows. The statistical solution of the model kinetic equation (BGK/ES-BGK) successfully captures the boundary layer and nozzle core flow as well. The NS solver produces results accurate in the core flow but strongly differs from the ES-BGK, DSMC and particle BGK throughout the boundary layer even with the imposition of velocity slip and temperature jump boundary conditions at the nozzle wall. It can be stated that NS prediction in the rarefied flow regime is inadequate and should not be used when an accurate solution of the flow over the nozzle lip is required, such as in contamination problems. These observations are consistent with the modeled boundary layer profiles obtained by the DSMC, the statistical BGK/ES-BGK, and NS methods, as will be discussed in Sec. III.C.

Having compared the supersonic flow expansion inside the nozzle, we now discuss the flow results in the backflow region downstream of the nozzle exit. Figure 4 shows the variation of axial velocity and temperature across a plane normal to the nozzle centerline at x/D of $\sim$0.85 downstream of the nozzle exit plane. In the same figures, the local Knudsen number based on density gradient ($Kn = \frac{\lambda d\rho}{\rho dx}$), is also shown. It can be clearly seen that the local Knudsen number shows a large increase at the nozzle lip (y/D=$\sim$4), increasing to a value greater than unity, and, thereby making the NS equations invalid for modeling the back flow region. From velocity and temperature profiles, as shown in Fig. 4, it can be seen that the statistical ES-BGK method shows very good agreement with the benchmark DSMC method for both axial velocity and temperature (with a maximum deviation of less than 5%), while the NS method shows significant deviation from the DSMC method. The disagreement between the NS and DSMC method is more than 30%, thereby making the use of NS method for such multiscale flow applications questionable. Using the back flowfield data, we computed the mass flow rate at the exit plane of the nozzle in the direction opposite to that of the nozzle core flow, and found that the statistical ES-BGK and DSMC methods provide a value of $\sim 7.5\times10^{-9}$ kg/s, while the NS solution does not predict any mass flow rate in the backward

direction. While it is true that the backwards mass flow rate is very small compared to the overall mass flow rate of $20.2\times10^{-6}$ kg/s through the nozzle, the flow rate is such that it cannot be ignored from the standpoint of spacecraft contamination.

All the aforesaid studies with respect to the particle BGK and ES-BGK methods were carried out with a cell size of 24 $\mu$m, a time step of $2\text{x}10^{-8}$s (satisfying the requirements of the DSMC method described in Sec. II.A) and about 150 number of particles per cell so as to eliminate the statistical error. Having demonstrated the effectiveness of the model kinetic equations in simulating a transitional micro nozzle flow, we discuss the numerical efficiency of particle BGK/ES-BGK methods in comparison to DSMC. To this end, sensitivity studies were carried out, wherein cell size, time step and number of particles in a cell are varied to reach an accurate and computationally most efficient solution. It was found that the mesh independent solution for particle BGK and ES-BGK methods can be obtained with a cell size of 80 $\mu$m, a corresponding time step of $1.5\text{x}10^{-8}$s and with an average number of about 40 particles in a cell rather than 150. It took about 6.5 hours for statistical BGK and ES-BGK methods to reach a converged state using 20 Intel 3GHz Xeon processors. In the use of DSMC, a mesh independent converged solution could be obtained with a maximum cell size of 40 $\mu$m, a time step of $1\text{x}10^{-8}$s, and with 15 particles in a cell. The solution required approximately 10 hours using the same computer hardware. We note that with these numerical parameters, the solutions obtained with the particle BGK/ES-BGK method agree well with those obtained from DSMC.

Table 1 shows the comparison of computational time required by the various methods to reach a mesh independent converged state for the low pressure case. The performance data for DSMC and statistical methods were obtained using Intel 3GHz Xeon processors, while Intel Itanium 2(1.6 GHz) processors were used for the FV ES-BGK and NS solver. It is evident that the particle BGK and ES-BGK methods require less CPU time than the DSMC method without incurring any loss in the accuracy of the solution. It can also be inferred that the cell size could be larger in the statistical BGK and ES-BGK methods compared to the DSMC method, which would allow us to use these methods for higher pressure cases, where DSMC cannot be used due to the high computational cost. It is interesting to note that the convergence process is quite different for DSMC and statistical BGK/ES-BGK methods. The DSMC method tends to reach steady state faster, but requires more computational effort to collect sufficient information for the solution to be smooth (i.e., sampling). On the other hand, statistical BGK/ES-BGK methods reach steady state slower (perhaps due to the "history" of the macroparameter sampling procedure which defines the local Maxwellian distribution function), but smoothness of the results is achieved earlier than in the case of DSMC (probably for the same reason). The most time efficient method is the NS method, however, at the cost of accuracy in the rarefied portion of the flow.

In summary for this case, we can conclude that the statistical and FV ES-BGK results are in good agreement with the DSMC solution in the entire diverging part of the nozzle. The statistical solution of the model kinetic equation accurately captures both the boundary layer and the nozzle coreflow with a significant saving in computational time over DSMC method. Even though the velocity slip and temperature jump boundary conditions were used at the wall in the case of NS, it fails to model the rarefaction effects and predict the proper macroparameter values in the boundary layer and at the nozzle lip.

### III.B. High pressure Case II

Results for the high pressure Case II were obtained with the baseline DSMC method, statistical BGK and ES-BGK schemes, FV ES-BGK solver, and the NS solver. Although the DSMC method is not usually applied for such a case due to significant computational requirements, we were able to obtain a mesh independent solution and satisfy all the DSMC numerical requirements. Similar to the low pressure case, Fig. 5 presents a comparison of the predicted spatial temperature distribution predicted by the DSMC, ES-BGK, and NS approaches. This and subsequent figures are normalized in the same manner as discussed in the previous section. The flow exhibits similar features, compared to the lower pressure case, of an inviscid core and a thick boundary layer. The higher stagnation pressure, however, causes the boundary layer to be thinner compared to the lower pressure case as can be seen by comparison of Figs. 5 and 1. Also, since the present case is for a pressure 10 times higher than for the low pressure case, the agreement between the solutions of the NS and DSMC method is better than in the lower pressure case, as expected. However as before, the agreement slightly worsens in the relatively rarefied portions of the flow, near the nozzle exit and close to the boundary layer.

To provide a quantitative evaluation, we now compare results of all of the numerical schemes in several linear plots presenting the velocity and temperature profiles along the nozzle center line (Fig. 6) and at the exit plane of the nozzle (Fig. 7). Figures 6 and 7 also present results of the eDSMC[20] solution for this high pressure case. The eDSMC calculations were computed using 0.85 million cells with 5 million particles. Figure 6 shows that the DSMC, NS, FV ES-BGK, statistical BGK, ES-BGK, and eDSMC predicted profiles for both velocity and temperature are close along the nozzle centerline. Because the nozzle throat region is modeled in our studies as a sharp corner, the flow develops a weak shock wave which is then reflected from the centerline. It can be seen that the DSMC, FV ES-BGK and NS methods were able to predict this feature of the flow, but the statistical BGK and ES-BGK methods slightly overpredict viscosity, diffusing this feature through the weak shock wave. The lack of prediction of the weak shock wave also accounts for some of the difference in the inviscid core seen between the DSMC and ES-BGK contours shown in Fig. 5. Across the

nozzle exit plane, as in case I, there is more variation in the velocity and temperature profiles among the different methods, as seen in Fig. 7. The figure shows that the eDSMC method predicts a velocity and thermal boundary layer profile significantly different from the other methods, with even small differences observed in the core region ($y/D < 2$) temperature profile. This disagreement is consistent with that observed in earlier work even though this high pressure case is a factor of ten more dense than was considered in Ref. 20. The results across the nozzle exit plane show that there is still some difference between the NS and DSMC predictions in both the temperature and flow velocity. As in the lower pressure case, this difference is explained by the limitations of the velocity slip and temperature jump boundary condition used in the NS. The remaining numerical methods all agree well with DSMC.

In a manner similar to the low pressure case, we now present the flowfield data in the back flow region for Case II. Figure 8 show the variation of the x component of velocity and temperature across a plane normal to the nozzle centerline at $x/D =\sim 0.85$ downstream of the nozzle exit plane. Again, the variation of local Knudsen number based on the density gradient, is shown in the figure and it can be seen that the variation is large in the nozzle lip region, even for a high pressure case. Similar to the low pressure case, the solution predicted by the NS equations deviates from that of DSMC. The figure shows that although there are regions with Knudsen number well within the continuum, deviation between the two solutions is significant, particularly, in the region where $Kn < 0.1$. The disagreement between the NS and DSMC is as much as 20% in both velocity and temperature, whereas the statistical ES-BGK method shows only a discrepancy of less than 4% from the DSMC, which is within the numerical accuracy. Once again, the back flow rate, calculated at the nozzle exit plane, predicted by the NS solution is zero, whereas both DSMC and ES-BGK methods predict a value of $\sim 18\times10^{-9}$ kg/s (compared to the total mass flow rate of $202.2\times10^{-6}$ kg/s through the nozzle).

Similar to the low pressure case, we carried out a sensitivity study for this case to demonstrate the numerical efficiency of the methods. Again, the performance data for the DSMC and statistical BGK/ES-BGK methods was obtained using Intel 3GHz Xeon processors, while Intel Itanium 2(1.6 GHz) processors were used for the FV ES-BGK and NS solver. It was found that it takes less time to reach a mesh independent converged solution using the particle BGK and ES-BGK methods compared to a DSMC converged solution. Table 2 shows the comparison of computational time required by the various methods for the high pressure case. It should be noted that the particle BGK and ES-BGK methods take less time compared to DSMC because the cell size requirement is relaxed in the BGK methods, although these methods require more particles per cell than DSMC. This case is perhaps the limiting maximum pressure case solvable by the DSMC method, with the present com-

putational power making it unfeasible to extend to higher pressures. Since the cell size requirement can be relaxed for the statistical BGK and ES-BGK methods, they can be used for higher pressure cases. The FV ES-BGK method takes a large amount of time, although, its results agree well with the DSMC method. The eDSMC method, although fast and comparable with the NS solver, does not capture the viscosity effects in the boundary layer as was suggested by earlier results discussed in Ref. 20. However the solution in the inviscid core of the flow is remarkably close to the solutions obtained by the other methods. The NS solver again turns out to be the most time efficient method, however at the cost of accuracy in the rarefied portions of the boundary layer.

### III.C. Comparison of Averaged Flow Quantities for Low and High Pressure Cases

We now discuss the averaged flow quantities, such as boundary layer thickness, displacement thickness and thrust, derived from the flowfield data obtained by the different methods. The boundary layer thickness, a function of distance along the centerline, is defined as that distance from the nozzle wall where the local flow velocity reaches 0.99 of the axial velocity.[32] Note that the presence of rarefaction causes the boundary layer thickness to deviate from the traditional slender body continuum square root of axial distance behavior. Figure 9 compares the boundary layer profiles obtained by the DSMC, NS and the statistical BGK and ES-BGK methods for the low and high pressure cases. It can be seen that the agreement between the statistical BGK/ES-BGK and DSMC methods is good, while, there is a noticeable difference between the NS and DSMC values. Table 3 shows a comparison of the boundary layer thickness at the nozzle exit obtained by the aforesaid methods for the low and high pressure cases. The percentage difference between the values of boundary layer thickness (at the nozzle exit) obtained from the NS and DSMC methods is on average about 8% for both pressure cases. The statistical BGK and ES-BGK methods show considerably good agreement DSMC with a maximum deviation of about 4.8% for the low and high pressure cases.

The displacement thickness is defined as the distance the undisturbed core flow is displaced from the boundary by a stagnant layer that removes the same mass flow from the flow field as the actual boundary layer, *i.e.,* it is the thickness of a zero velocity layer that has the same mass-flow defect as the actual boundary layer.[32] Table 4 shows a comparison of the displacement thickness at the nozzle exit for the aforesaid methods for the low and high pressure cases. It is worth noticing that the NS solution results in a significantly different displacement thickness values relative to DSMC as compared to the other methods. The percentage difference between the NS and DSMC values is greater than $\sim 40\%$ for both low and high pressure cases. On the other hand, the statistical BGK/ES-BGK methods show

good agreement with the DSMC methods with a maximum disagreement of $\sim 4.5\%$ for the low and high pressure cases. From Tables 3 and 4, it can be inferred that the statistical methods resolve the boundary layer quite well, which in turn would suggest that they will be useful for accurately predicting other derived flow parameters such as thrust as discussed below.

Using the flow field data, thrust was computed for the DSMC, statistical BGK/ES-BGK and NS methods. Table 5 compares the thrust values obtained for the different methods using their respective flow field data for both low and high pressure cases. It should be noted that the percentage difference between the thrust values obtained from the different methods is less than 3% for both low pressure and high pressure cases. The maximum disagreement of 3% is observed between NS and DSMC solutions for the low pressure case. The thrust is a spatially averaged quantity that includes the core and boundary layer portions of the flow. Since the inviscid core flow, particularly at higher Reynolds numbers, spatially dominates the average, the thrust agreement between different methods is better than that computed for the boundary layer thickness. The statistical methods provide an accurate alternative to NS for predicting micro-nozzle thrust, but, at a significant computational cost. However, even though the NS solution provides a reasonably accurate prediction of thrust, it fails to model the back flow correctly as was shown in Figs. 4 and 8 for the low and high pressure cases, respectively. The numerical advantage associated with the statistical ES-BGK methods, compared to DSMC, together with its accuracy, makes it a preferable method for modeling multi-scale flows, involving contaminant back flow, where in particular, DSMC method may not be usable at high pressures.

## IV. Conclusions

Argon flow through a conical nozzle was studied for two Reynolds numbers of 1,230 and 12,300, using four different approaches. These include a continuum approach, solution of Navier-Stokes equations, and three kinetic approaches, the DSMC method, and statistical and deterministic methods for the BGK/ES-BGK equations. Analyses of the accuracy of the approaches and their numerical efficiency were conducted for supersonic expansions to vacuum nozzle flows. These cases were selected because they span the range of conditions found in micro-nozzle flows. Since the DSMC numerical parameters were chosen to ensure that its solutions were independent of the numerical parameters for both the high and low pressure cases, it was considered truth in the comparison with the other gas dynamic approaches. Several conclusions can be drawn from the results of the computations. The statistical and finite volume solution of the BGK and ES-BGK equations are in a good agreement with the DSMC method in the entire computational domain for both Reynolds numbers. Statistical

BGK and ES-BGK methods save computational time compared to DSMC without incurring any loss in the accuracy of the solution. Also it was found that the statistical BGK/ES-BGK methods did not require the use of the strict DSMC numerical criteria, as described in Sec. II.A, and therefore are more likely candidates for use in multi-scale, high pressure cases, where the use of the DSMC method is either not possible or not practical. The eDSMC method was not able to reproduce the viscosity effects in the boundary layer, although, because the solution in the inviscid core is good it could be used in a hybrid approach.

The Navier-Stokes solutions are computationally the most tractable and are in a good agreement with the DSMC results in the higher density core portion of the flow where rarefaction effects are small. In the boundary layer, however, even though the velocity slip and temperature jump boundary conditions were used, there is a noticeable difference between the NS and DSMC solutions. Although the NS method results in a reasonably accurate thrust prediction, it fails to model correctly the back flow beyond the nozzle exit, which is important when contamination of mission critical systems from onboard spacecraft nozzle systems must be avoided.

## Acknowledgments

The research being performed at the Pennsylvania State University is supported by the Air Force Office of Scientific Research Grant No.F49620-02-1-0104, whose support is gratefully acknowledged. Special thanks are to Professor M. Ivanov of the Institute of Theoretical and Applied Mechanics, Novosibirsk, Russia for the use of the original SMILE code.

## References

[1]Titov, E., A.Gallagher-Rogers, Levin, D., and Reed, B., "Examination of a Collision-limiter, DSMC Method for Predicting Micro-propulsion Thruster Performance," *Journal of Propulsion and Power*, Vol. 24, 2008, pp. 311–321.

[2]Pisacane, V., *The Space Environment and Its Effects on Space Systems*, American Institute of Aeronautics and Astronautics, 2008.

[3]Arnold, G. S., "Spacecraft Contamination Model Development," *SPIE Conference on Optical System Contamination: Effects, Measurements, and Control VI, San Diego, CA*, Vol. 3427.

[4]Vashchenkoiv, P., Kudryavtsev, A., Khotyanovsky, D., and Ivanov, M., "DSMC and Navier-Stokes Study of Backflow for Nozzle Plumes Expanding into Vacuum," *RGD24 International Symposium on Rarefied Gas Dynamics*, 2005.

[5]Bird, G. A., *Molecular Gas Dynamics and the Direct Simulation of Gas Flows*, Clarendon Press, Oxford, 1994.

[6]Xie, C., "Characteristics of micronozzle gas flows," *Physics of Fluids*, Vol. 19, No. 3, 2007, pp. 037102.

[7]San, O., Bayraktar, I., and Bayraktar, T., "Size and expansion ratio analysis of micro nozzle gas flow,"

*International Communications in Heat and Mass Transfer*, Vol. 36, No. 5, May 2009.

[8]Gimelshein, S., Alexeenko, A., and Levin, D., "Modeling of the interaction of a side jet with a rarefied atmosphere." *Journal of Spacecraft and Rockets*, Vol. 39, No. 2, 2002, pp. 168–176.

[9]Gimelshein, N., Lyons, R., Reuster, J., and Gimelshein, S., "Numerical Prediction of UV Radiation from Two-Phase Plumes at High Altitudes," *AIAA Journal*, Vol. 46, No. 7, 2008, pp. 1764–1772.

[10]Torre, F. L., Kenjeres, S., Kleijn, C., and Moerel, J., "Evaluation of Micronozzle Performance through DSMC, Navier-Stokes and Coupled DSMC/Navier-Stokes Approaches," *Book Series Lecture Notes in Computer Science*, Vol. 5544/2009, May 2009, pp. 675–684.

[11]Eggers, J., "New algorithms for application in the direct simulation Monte Carlo method," *In Rarefied Gas Dynamics: Theory and Simulations, ed. BD Shizgal, DP Weaver, Progress in Astronautics and Aeronautics*, Vol. 159, 1994, pp. 166–173.

[12]Roveda, R., Goldstein, D., and Varghese, P., "Hybrid Euler/particle approach for continuum/rarefied flows," *J Spacecraft Rockets*, Vol. 35, 1998, pp. 258–265.

[13]Arslanbekov, J. R., Kolobov, V., and Gimelshein, S., "Testing of the Unified Flow Solver (UFS) for Nozzle and Plume Flows," *AIAA Paper 2007-209*.

[14]Bourgat, J., Tallec, P., and Tidriri, M., "Coupling Boltzmann and Navier-Stokes Equations by friction," *Journal of Computational Physics*, , No. 127, 1996, pp. 227–245.

[15]Bhatnagar, P., Gross, E., and Krook, M., "A model for collision processes in gases," *Physical Review*, Vol. 94, 1954, pp. 511.

[16]Gallis, M. A. and Torczynski, J. R., "The Application of the BGK Model in Particle Simulations," *AIAA Paper No. 2000-2360, 34th AIAA Thermophysics Conference, Denver Co.*, June 2000.

[17]Nanbu, K., Igarashi, S., and Watanabe, Y., "Stochastic solution method of the model kinetic equation for diatomic gas," *Journal of the Physical Society of Japan*, Vol. 57, 1954, pp. 3371–3375.

[18]Burt, J. M. and Boyd, I. D., "Evaluation of a Particle Method for the Ellipsoidal Statistical Bhatnagar-Gross-Kroook Equation," *44th AIAA Aerospace Science Meeting and Exhibit, AIAA Paper 2006-989, Reno, Nevada*, January 2006.

[19]Burt, J. and Boyd, I., "Extension of a Mutliscale Particle Scheme to Near-Equilibrium Viscous Flows," *AIAA Journal*, Vol. 47, No. 6, 2009, pp. 1507–1517.

[20]Titov, E. and Levin, D., "Extension of the DSMC method to high pressure flows," *Journal of Computational Fluid Dynamics*, Vol. 21, 2007, pp. 351.

[21]Holway, L., "Kinetic Theory of Shock Structure using Ellipsiodal Distribution Function," *Rarefied Gas Dynamics: Proceedings of the 4th International Symposium, University of Toronto*, Vol. 1, 1996, pp. 193–215.

[22]Ivanov, M. and Gimelshein, S., "Current Status and Prospects of the DSMC Modeling of Near-Continuum Flows of Non-reacting and Reacting Gases," *Proceedings of the Rarefied Gas Dynamics 23rd Int. Symp., AIP Conference*, Vol. 663, 2003, pp. 339–348.

[23]Ivanov, M. and Rogasinsky, S., "Analysis of numerical techniques of the direct simulation Monte Carlo method in the rarefied gas dynamics," *Soviet Journal of Numerical Analysis and Mathematical Modeling*, Vol. 3, No. 6, 1988, pp. 453–465.

[24]"CFD++ User Manual Version 5.1.1," 2005.

[25]Macrossan, M., "A Particle Simulation Method for the BGK Equation," *Proceedings of the 22 International Symposium on Rarefied Gas Dynamics*, 2001, pp. 426–433.

[26]Holway, L., "Kinetic Theory of Shock Structure using Ellipsoidal Distribution Function," *Proceedings of the Fourth Internation Symposium on Rarefied Gas Dynamics*, 1966, pp. 193–215.

[27]Cercignani, C., "The Boltzmann Equation and its Applications," *Applied Mathematical Sciences*, 1988.

[28]Andries, P. and Perthame, B., "The ES-BGK Model Equation with Correct Prandtl Number," *Proceedings of the 22nd International Symposium on Rarefied Gas Dynamics, American Institute of Physics*, 2001, pp. 426–433.

[29]Mieussens, L., "Discrete-Velocity Models and Numerical Schemes for the Boltzmann-BGK Equation in Plane and Axisymmetric Geometries," *Journal of Computational Physics*, Vol. 162, 2000, pp. 429–466.

[30]Rothe, D. E., "Electron-Beam Studies of Viscous Flows in Supersonic Nozzles," *AIAA Journal*, Vol. 9, 1971, pp. 809–811.

[31]Ivanov, M. S., Markelov, G. N., and Gimelshein, S. F., "Statistical simulation of reactive rarefied flows: numerical approach and application," *AIAA Paper 98-2669*, June 1998.

[32]Currie, I. G., *Fundamental Mechanics of Fluids Third Ed.*, Marcel Dekker, Inc., 2003.

**Table 1. Efficiency of the methods, Low Pressure Case I**

| Method | DSMC | Part BGK | Part ES-BGK | FV ES-BGK | NS |
|---|---|---|---|---|---|
| Time (CPUH) | 200 | 130 | 130 | 400 | <1 |
| Num. of Particles (million) | 15 | 4.67 | 4.67 | - | - |
| Num. Cells | 3,000,000 | 120,000 | 120,000 | 3,600 | 3,600 |

**Table 2. Efficiency of the methods, High Pressure Case II**

| Method | DSMC | Part BGK | Part ES-BGK | FV ES-BGK[a] | NS |
|---|---|---|---|---|---|
| Time (CPUH)[b] | 1000 | 840 | 840 | 5000 | <3 |
| Number of Particles (million) | 75 | 50 | 50 | - | - |
| Number of Cells | 15,000,000 | 1,260,000 | 1,260,000 | 17,00 | 14,400 |

[a]FV ES-BGK times are for spatial-velocity grid converged results

[b]The times reported for the first three methods are for a 3GHz Xeon processor, while the last two are for a Intel Itanium 2(1.6 GHz) processor.

**Table 3. Comparison of boundary layer thickness (mm) at the nozzle exit, Case I, II**

| Case | DSMC | Particle BGK | Particle ES-BGK | NS |
|---|---|---|---|---|
| Re=1230 (Case I) | 7.73 | 8.09 | 7.83 | 7.20 |
| Re=12300 (Case II) | 5.96 | 6.25 | 6.14 | 5.40 |

**Table 4. Comparison of displacement thickness (mm) at the nozzle exit, Case I, II**

| Case | DSMC | Particle BGK | Particle ES-BGK | NS |
|---|---|---|---|---|
| Re=1230 (Case I) | 6.47 | 6.19 | 6.42 | 3.66 |
| Re=12300 (Case II) | 3.34 | 3.18 | 3.23 | 1.87 |

**Table 5. Comparison of nozzle thrust (mN), Case I, II**

| Case | DSMC | Particle BGK | Particle ES-BGK | NS |
|---|---|---|---|---|
| Re=1230 (Case I) | 9.85 | 9.77 | 9.81 | 9.55 |
| Re=12300 (Case II) | 1.12 | 1.10 | 1.11 | 1.10 |

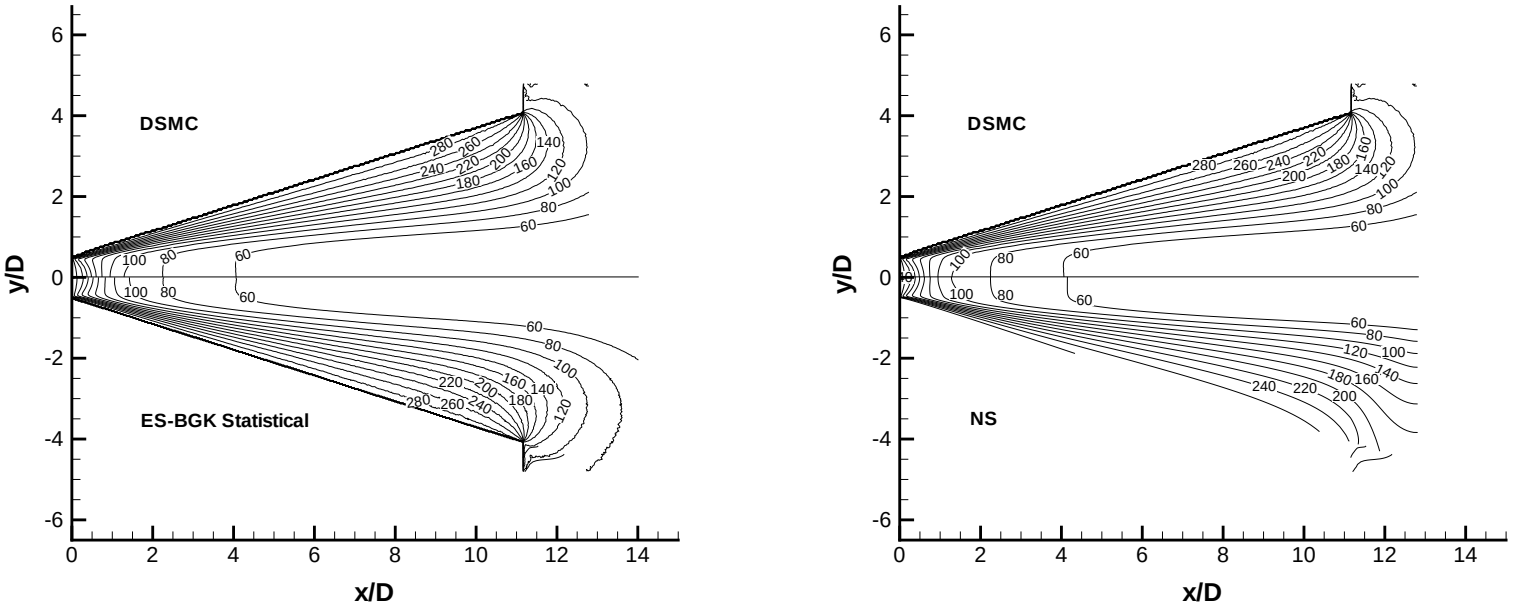


(a) Statistical ES-BGK vs. DSMC (b) NS vs. DSMC

**Figure 1. Case I, comparison of temperature [K] contours for different flow methods.**

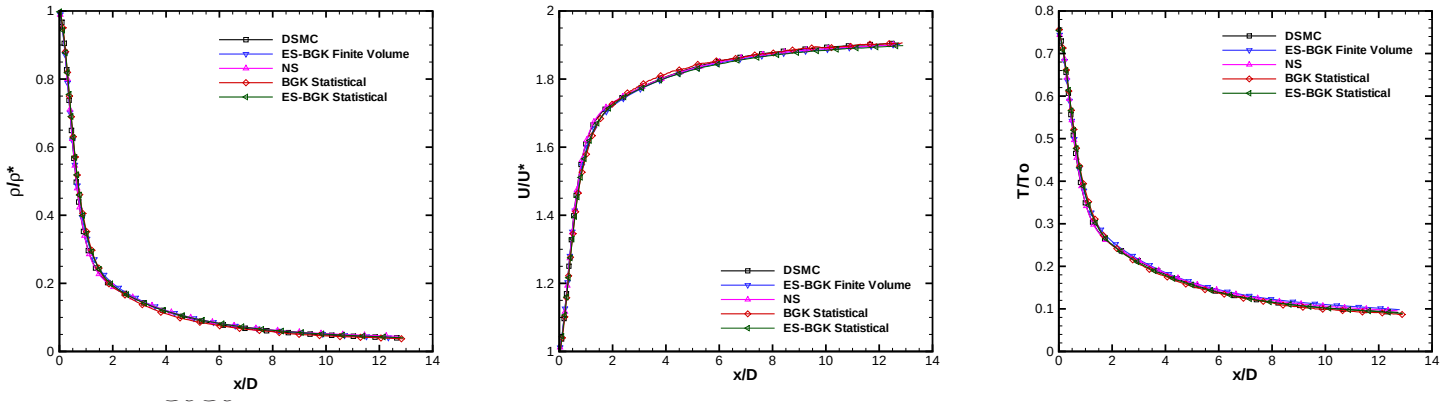


(a) Density (b) X component velocity (c) temperature (K)

**Figure 2. Case I, comparison of nozzle centerline macro-parameters for different gas dynamic techniques.**

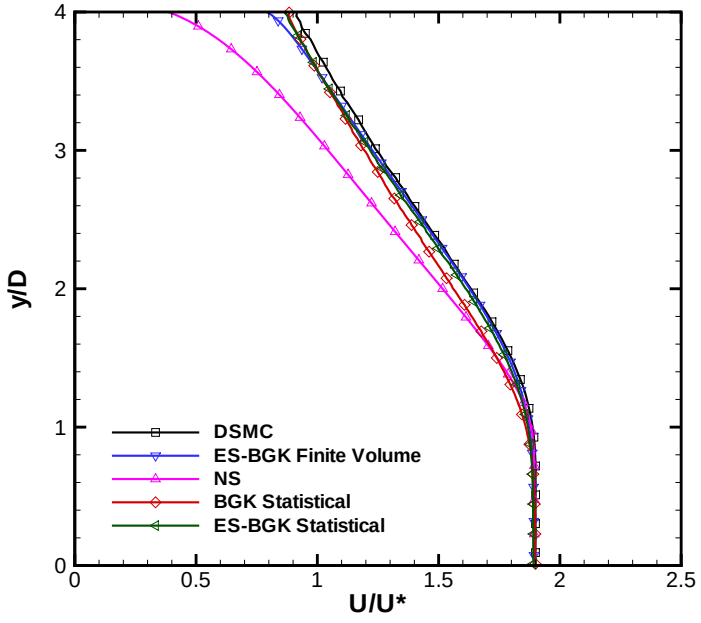


(a) X component velocity

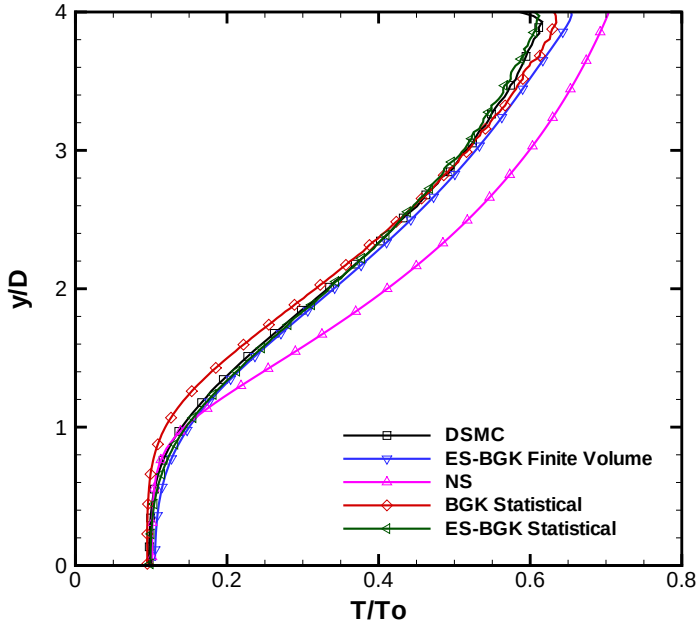


(b) Temperature

**Figure 3.** Case I, comparison of velocity and temperature profiles across the nozzle exit for different gas dynamic approaches.

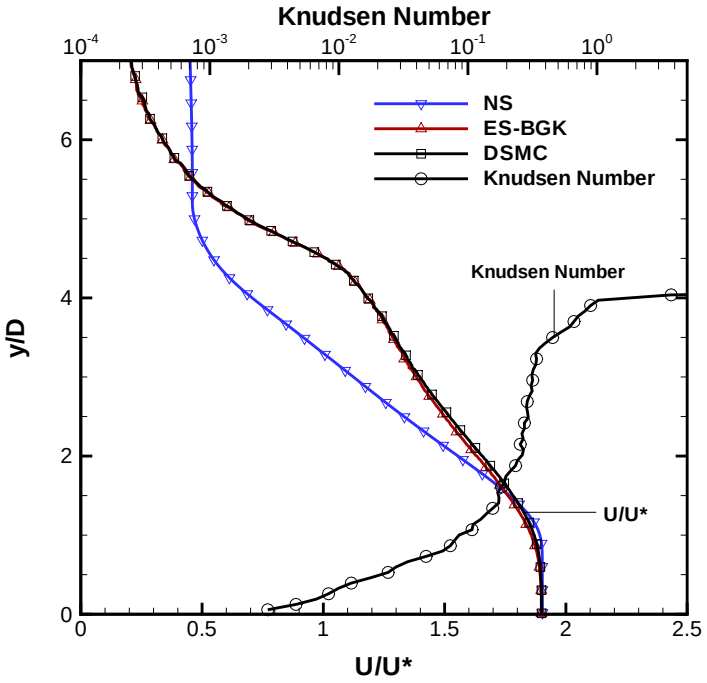


(a) X component velocity

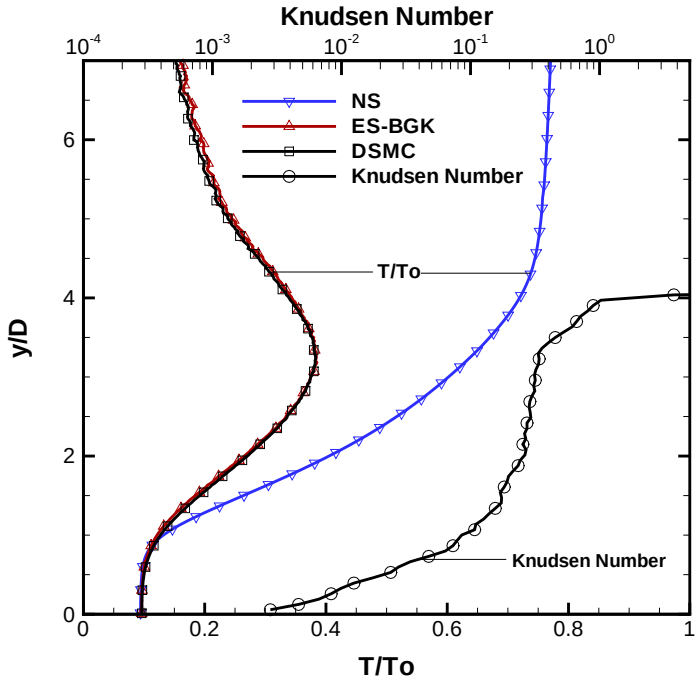


(b) Temperature

**Figure 4.** Case I, comparison of velocity, temperature, and local Knudsen number profiles across a plane normal to the nozzle centerline at a location of x/D~0.85 beyond the nozzle exit for different gas dynamic approaches.

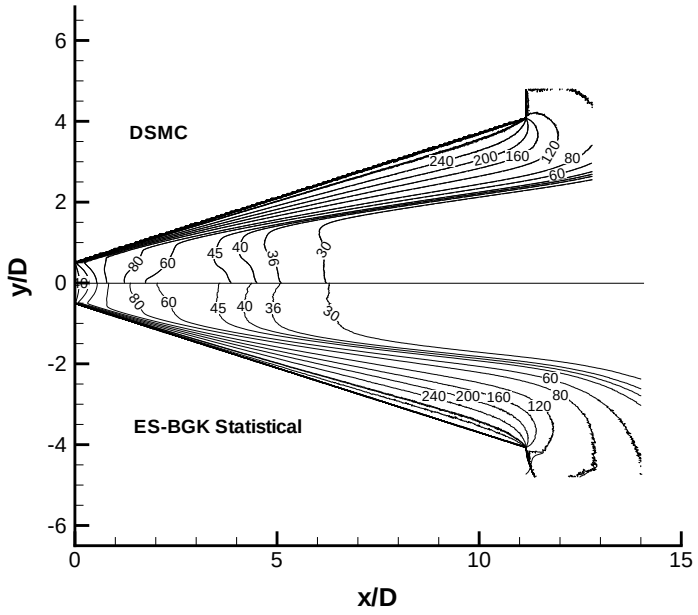


(a) Statistical ES-BGK vs.DSMC

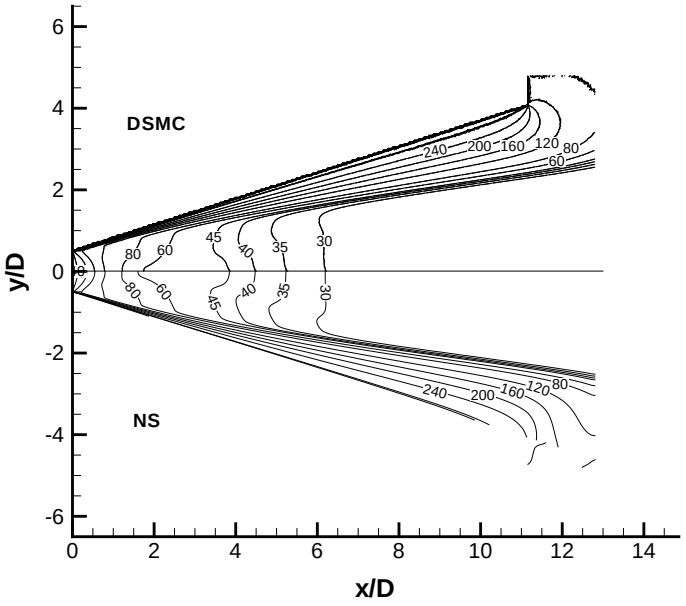


(b) NS vs. DSMC

**Figure 5. Case II, comparison of temperature [K] contours for different flow methods.**

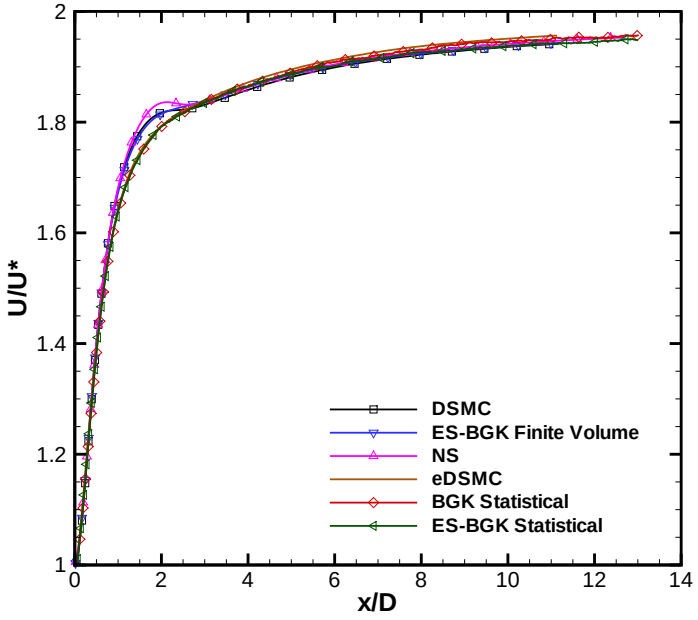


(a) X component of velocity

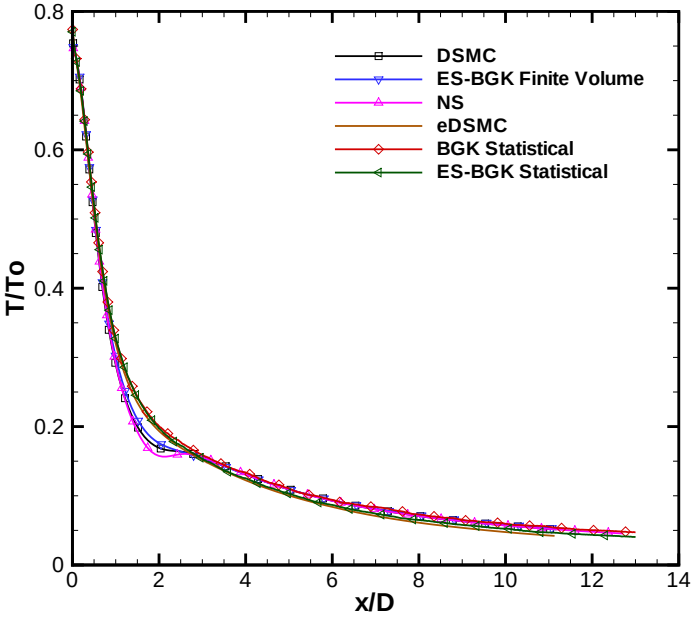


(b) Temperature

**Figure 6. Case II, comparison of nozzle centerline macro-parameters for different gas dynamic techniques. Case II, X component velocity profile along the nozzle centerline**

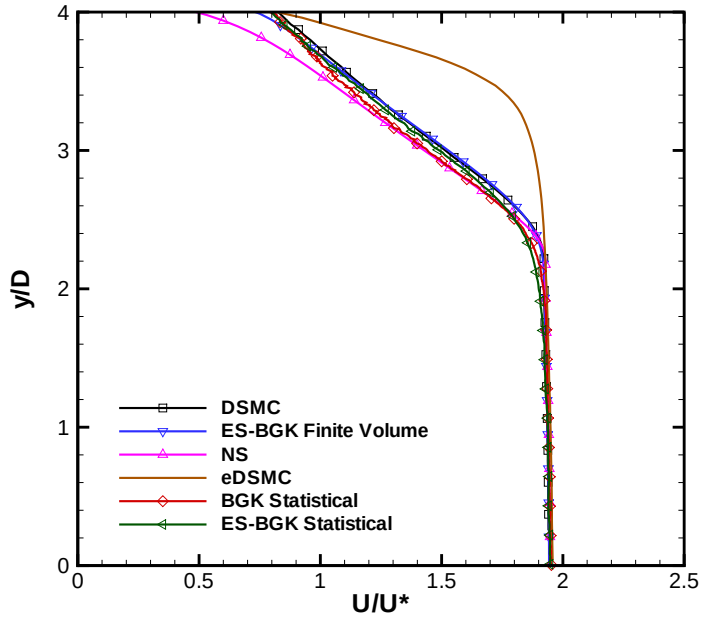


(a) X component of velocity

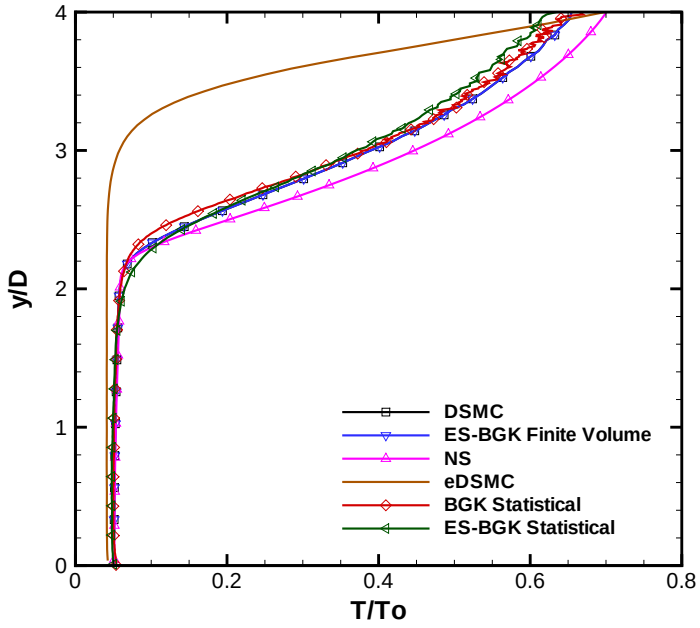


(b) Temperature

**Figure 7.** Case II, comparison of velocity and temperature profiles across the nozzle exit for different gas dynamic approaches.

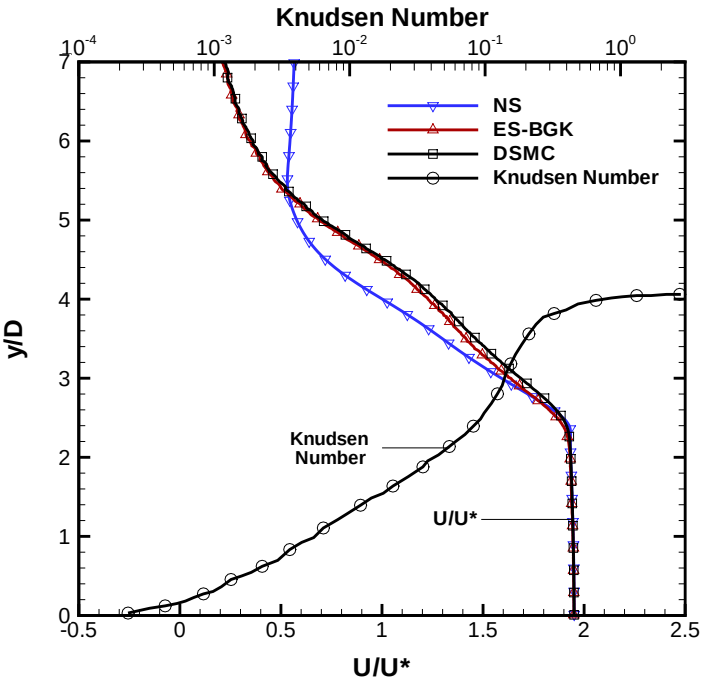


(a) X component velocity

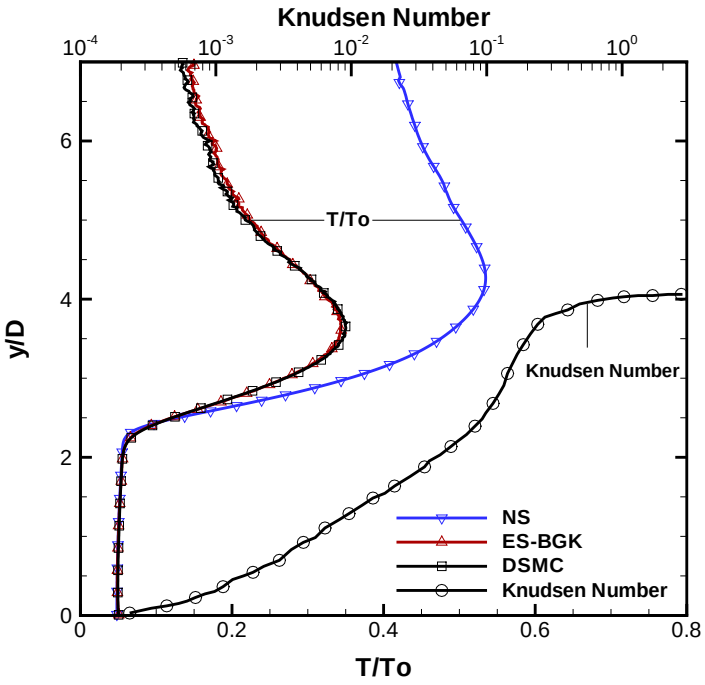


(b) Temperature

**Figure 8.** Case II, comparison of velocity, temperature, and local Knudsen number profiles across a plane normal to the nozzle centerline at a location of x/D∼0.85 beyond the nozzle exit.

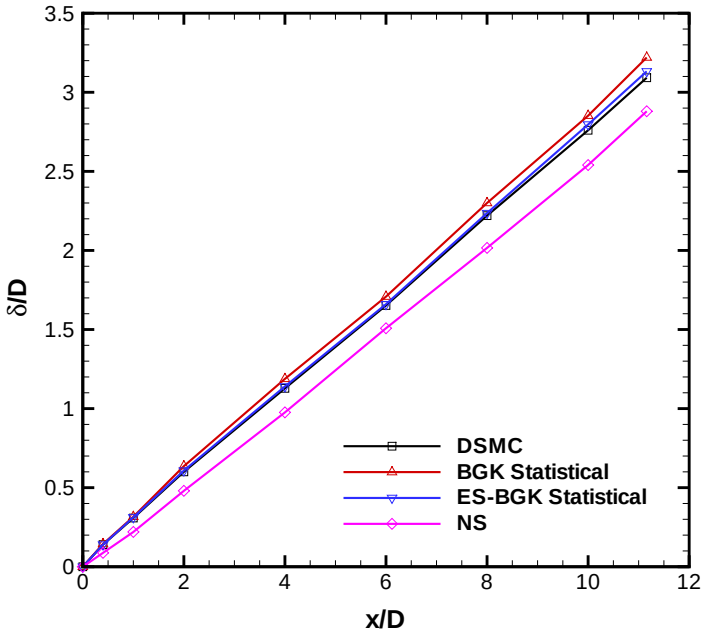


(a) Case 1

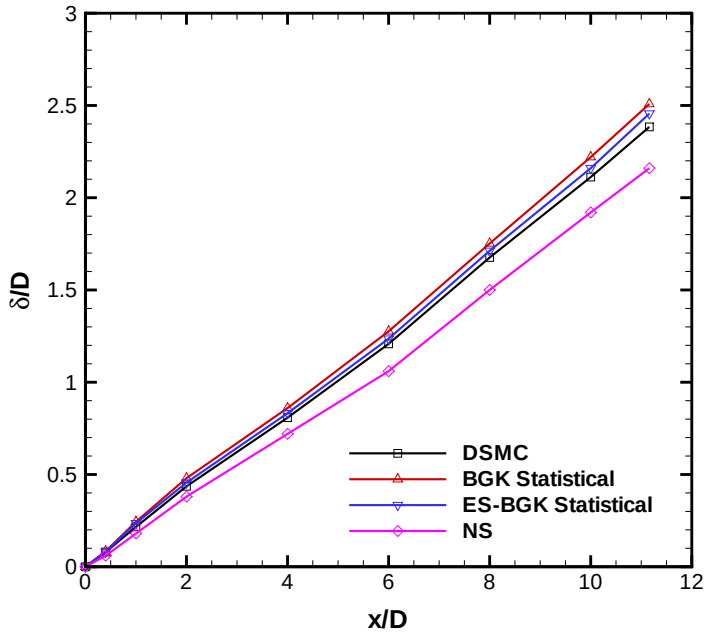


(b) Case II

**Figure 9. Comparison of growth of the boundary layer thickness along the nozzle for the low and high pressure cases.**